Catal Lett (2012) 142:1049–1056
DOI 10.1007/s10562-012-0869-2

ORIGINAL ARTICLES

Reactivity of Ga_2O_3 Clusters on Zeolite ZSM-5 for the Conversion of Methanol to Aromatics

Jose A. Lopez-Sanchez · Marco Conte · Phil Landon · Wu Zhou · Jonathan K. Bartley · Stuart H. Taylor · Albert F. Carley · Christopher J. Kiely · Karim Khalid · Graham J. Hutchings

Received: 10 May 2012 / Accepted: 28 June 2012 / Published online: 18 July 2012

Abstract Composites of Ga_2O_3 clusters and zeolite ZSM-5 were evaluated for the transformation of methanol to hydrocarbons. Comparison of the activity with ZSM-5 showed that the Ga_2O_3 clusters are responsible for the enhanced selectivity to aromatics via contact synergy, thus showing the importance of non framework gallium species for this reaction. TEM analysis of fresh and spent catalysts allowed the identification of the formation of carbonaceous products at the Ga_2O_3/zeolite interface region, and this interface is also the probable location of the catalyst active sites.

Keywords Gallium oxide · ZSM-5 · Methanol · Aromatics

J. A. Lopez-Sanchez · M. Conte · P. Landon · J. K. Bartley · S. H. Taylor · A. F. Carley · G. J. Hutchings (✉)
Cardiff Catalysis Institute, School of Chemistry, Cardiff University, Main Building, Park Place, Cardiff CF10 3AT, UK
e-mail: hutch@cf.ac.uk

Present Address:
J. A. Lopez-Sanchez
The Department of Chemistry, Stephenson Institute for Renewable Energy, University of Liverpool, Liverpool L69 7ZD, UK

W. Zhou · C. J. Kiely
Department of Materials Science and Engineering, Lehigh University, 5 East Packer Avenue, Bethlehem, PA 18015-3195, USA

K. Khalid
SABIC Technology & Innovation, P.O. Box 42503, Riyadh 11551, Saudi Arabia

1 Introduction

Zeolites are known to convert methanol to a wide range of hydrocarbons, including gasoline [1], olefins [2] and aromatics [3]. However, one of the major targets remaining is to maximise the selectivity to aromatic products using simple and highly reproducible catalyst preparation routes. Ga/ZSM-5 is a widely used catalyst to convert methanol to hydrocarbons, especially aromatic products, and it is typically prepared using gallium nitrate precursors dissolved and impregnated onto ZSM-5 [4]. However, despite the apparent simplicity, the impregnation of a zeolite with metal precursors is a complex process that can lead to the formation of metal or oxide nanoparticles, either inside or outside the zeolite pores [5, 6], and can generate framework or non framework gallium species [7]. However, during the synthesis most attention has focused on the reduction of Ga_2O_3 clusters [8] to generate Ga_2O species, which in turn can migrate into the zeolite channels leading to cationic gallium species like: Ga^{3+}, GaH^{+} or $GaH_2{}^{+}$ [9, 10]. This has led to catalysts capable of producing enhanced selectivity to aromatics in the methanol to hydrocarbons process [11–13]. In contrast, in the current work we wanted to specifically focus on the activity of extra framework species, like Ga_2O_3 on the external surface of the zeolite crystals, as to date this has received limited attention for the methanol to aromatics reaction [14]. Our aim is to consider the effect of competition between the basic sites of the metal oxide with the acid sites of the zeolite, as the former are postulated as responsible for dehydrogenation [15], and the latter for dehydration [1]. Our approach was to investigate the effect of Ga_2O_3 clusters supported on ZSM-5, by investigating catalysts prepared by impregnation from Ga solutions and from physical mixtures of Ga_2O_3 and ZSM-5.

2 Experimental

2.1 Catalyst Preparation

NH_4-ZSM-5 (Zeolyst SiO_2/Al_2O_3 mol ratio 30:1) was calcined at 550 °C in static air for 4 h (temperature ramp 20 °C/min) in order to obtain H-ZSM-5. The zeolite precursor (2 g) was physically mixed with β-Ga_2O_3 (Aldrich, 2 g) by grinding with a mortar and pestle for 2 min (final gallium content = 37 wt%).

$Ga(NO_3)_3 \cdot xH_2O$ (Aldrich, 1.508 g, assay 18.73 wt%) was dissolved in deionised water (25 mL) and mixed with untreated NH_4-ZSM-5 (Zeolyst, SiO_2:Al_2O_3 = 30; 4 g). The resulting slurry was heated slowly to 80 °C and evaporated to dryness. The catalyst was dried at 110 °C for 16 h, and calcined at 550 °C for 4 h in static air (temperature ramp 20 °C min^{-1}). The calculated Ga metal loading is 7.09 wt%.

2.2 Catalytic Tests and Characterization of the Products

All the catalysts were tested in pelleted form, obtained by pressing the solids twice at 2 tons cm^{-2} for 1 min. The pellets were then ground and sieved, collecting the fraction with particle diameters between 850 and 600 μm. Catalytic tests for the methanol to aromatics reaction were carried out using a glass reactor (i.d. = 9 mm) at 450 °C under Ar flow (60 mL min^{-1}) with a methanol feed of 320 μL h^{-1} over 0.125 g of catalyst for up to 12 h time on stream. Prior to the start of the reaction, all catalysts were pre-treated in air at 500 °C for 1 h. The reaction mixture was analysed via gas chromatography using a Varian CP-3800 Gas Chromatograph and a Varian CP-SIL8CB wide bore capillary column (60 m, 0.53 mm i.d., 1.5 μm film thickness) and Ar as carrier gas. Quantification of the hydrocarbons was carried out using a flame ionization detector (FID), while H_2 was quantified using a thermal conductivity detector (TCD). With our chromatographic method, it was possible to identify a ratio ethylene/ethane of ca. 18 and propene to propane of ca. 2. For the other classes of compounds, it was not possible to resolve alkanes to the corresponding alkenes with the analytical method. All the catalytic tests were carried out at a constant WHSV of 1.4 h^{-1} for comparative purposes.

2.3 Characterization Methods

X-ray powder diffraction patterns were acquired using an X'Pert PanAlytical diffractometer with a CuK_α source operating at 40 kV and 40 mA. Analysis of the patterns was carried out using X'Pert HighScore Plus software. Unit cell parameters were determined using Rietveld refinement as a full-pattern fit algorithm for the catalyst, and the agreement of fit between experimental and simulated XRPD patterns was evaluated via the χ^2 test. Initial atomic coordinate values to perform the fitting were obtained using crystallographic information files (CIF) available at the Database of Zeolite Structures (IZA-SC) for ZSM-5 and the Inorganic Crystal Structure Database (ICSD-WWW) for Ga_2O_3. The experimental errors for the unit cell lengths a, b, and c obtained from the Rietveld refinement were $\delta a = 0.010$ Å, $\delta b = 0.010$ Å and $\delta c = 0.008$ Å, thus leading to an experimental error of the unit cell volume of $\delta V = 0.16$ %.

Crystallinity was calculated from the XRPD patterns using a constant background intensity algorithm [16] and ZSM-5 as a calibration standard. In our case, imposing ZSM-5 as a 100 % crystalline phase, the corresponding crystallinity values for Ga_2O_3/ZSM-5 and WI-ZSM-5 were 99.7 and 99.5 % respectively.

Crystallite size was determined using the Scherrer equation [17] using the (011) reflection at 7.92° 2θ assuming spherical particles shapes and a K factor of 0.89.

Samples were prepared for transmission electron microscopy analysis by dry dispersing the catalyst powders onto a lacey-carbon film supported on a 300-mesh Cu TEM grid. Bright-field (BF) imaging and selected-area diffraction patterns were acquired using a JEOL 2000FX TEM operating at 200 keV with a LaB_6 filament.

Thermal gravimetric analysis (TGA) was performed using a Setaram Labsys TG–DTA/DSC 1600 instrument. The sample was heated from 30 to 700 °C in air at a rate of 10 °C min^{-1}, supported in an Al_2O_3 crucible. Combustion of carbonaceous product for samples after reaction occurred at ca. 500 °C and these were referenced with samples before reaction, where weight loss from adsorbed water only was detected.

3 Results and Discussion

To evaluate the effect of Ga_2O_3 systematically, physical mixtures of Ga_2O_3 and ZSM-5 were prepared, and their catalytic activity at 400 °C was compared with H-ZSM-5 (Tables 1, 2, 3). For all catalysts the conversion is always ca. 100 % as it is our aim to optimise the yield of aromatic products at complete conversion, therefore focusing on the selectivity. However, while ZSM-5 is only capable of ca. 25 % selectivity to aromatics within the total C_6–C_{10} fraction, the physical mixture of Ga_2O_3/ZSM-5 produced ca. 40 % aromatics under the same conditions. Control tests, using Ga_2O_3 only, did not display any catalytic activity, thus confirming the existence of a synergistic effect between Ga_2O_3 crystallites and ZSM-5. The impregnation method also has an important influence on catalyst activity,

Table 1 Methanol conversion over H-ZSM-5 (SiO_2:Al_2O_3 = 30:1)

Time (min)	Selectivity (wt%)										Total aromatics
	C_2	C_3	C_4	C_5	C_6+	C_6H_6	C_7H_8	C_8H_{10}	C_9H_{12}	$C_{10}H_{14}$	
34	14.3	28.8	20.6	5.4	0.5	1.4	6.2	4.3	0.9	0	12.8
65	13.9	27.7	19.7	3.8	0.5	1.5	6.7	14.3	0.6	0	23.2
98	13.8	28.3	21.5	5.2	0.5	1.4	6.4	13.8	4.1	0	25.8
129	15.9	27.1	20.0	5.7	0.4	1.5	6.4	14.0	4.8	0	26.9
162	15.8	27.7	20.4	4.8	0.4	1.6	6.6	13.3	4.8	0	26.4
193	14.3	26.6	19.5	5.7	0.4	1.6	6.8	14.6	4.7	0	27.9
274	13.9	26.0	18.1	5.7	0.4	1.7	7.0	15.2	5.3	0	29.2

Table 2 Methanol conversion over β-Ga_2O_3/H-ZSM-5 (SiO_2:Al_2O_3 = 30:1)

Time (min)	Selectivity (wt%)										Total aromatics
	C_2	C_3	C_4	C_5	C_6+	C_6H_6	C_7H_8	C_8H_{10}	C_9H_{12}	$C_{10}H_{14}$	
33	13.5	24.5	11.9	4.4	2.1	0.5	2.4	14.4	20.9	5.5	43.6
65	14.4	24.8	13.6	5.2	2.6	0.5	1.8	13.4	18.7	5.0	39.5
96	14.5	24.8	13.2	5.0	2.4	0.5	1.8	13.6	18.7	5.4	40.1
133	14.9	25.8	13.5	5.1	2.5	0.5	1.8	13.2	17.6	5.1	38.1
164	14.5	24.8	12.8	5.0	2.4	0.5	1.8	13.6	19.2	5.4	40.5
202	14.8	25.7	14.1	5.4	2.7	0.5	2.0	12.4	17.4	4.9	37.2

Table 3 Methanol conversion over impregnated Ga/H-ZSM-5

Time (min)	Selectivity (wt%)										Total aromatics
	C_2	C_3	C_4	C_5	C_6+	C_6H_6	C_7H_8	C_8H_{10}	C_9H_{12}	$C_{10}H_{14}$	
34	13.9	17.2	10.9	1.4	0	5.0	13.8	17.2	7.9	0	51.2
65	13.4	16.6	11.7	1.8	0	3.9	11.5	15.6	7.0	0	51.1
98	17.2	18.1	13.9	2.5	0	3.5	11.7	17.1	8.1	0	44.6
129	14.1	19.1	13.7	2.6	0	3.3	11.0	16.7	7.1	0.2	42.1
162	14.6	18.6	13.1	2.5	0	3.3	10.8	16.5	8.0	0.3	43.3
193	14.2	16.9	11.6	2.2	0	3.5	11.3	17.9	9.0	0.3	44.4
274	14.6	17.9	12.3	2.4	0	3.3	10.8	17.0	8.3	0.4	41.2

as Ga/ZSM-5 prepared by wet impregnation (WI) has a greater selectivity to aromatics of about 50 %.

A more detailed analysis of the data, considering the classes of compounds identified, also show a different product distribution within the aromatic products. In fact while ZSM-5 is capable of forming a significant amount of toluene (C_7H_8), (ca. 6 %, Table 1), the physical mixture of Ga_2O_3/ZSM-5 showed decreased toluene selectivity to ca. 2 %. However, the physical mixture increased, by almost four times, the C_9H_{12} fraction (ethyl methyl benzene isomers, Table 2) as well as promoting the formation of $C_{10}H_{14}$ (durene) isomers. This trend can be explained assuming a dehydrogenation reaction pathway triggered by Ga_2O_3 clusters [18]. It should be highlighted that durene is a compound that is often found in the methanol to hydrocarbons process and its formation is usually ascribed to alkylation of lower molecular weight aromatics with methanol [19], and it is also one of the components that contributes to coke formation [20]. In our case, when ZSM-5 only was used, no durene was detected, and TGA determination of the carbon content for this material was in the range of 0.2 %. In contrast, in the case of Ga_2O_3/ZSM-5 the amount of durene was ca. 5 % and the amount of coke was in the range of 5 % wt. This correlates well with the accepted models of durene and coke formation [21].

In addition, whilst coke formation decreased the selectivity to aromatics with time on stream, the conversion of methanol was always in the range of 100 %. It is also interesting to note how for the Ga/ZSM-5 zeolite prepared by impregnation (Table 3) an intermediate product distribution, between that of ZSM-5 alone and Ga_2O_3/ZSM-5, was evident with the exception of an enhanced selectivity to benzene up to ca. 5 %.

However, because methanol conversion was always 100 % and the aromatics are not primary reaction products, the catalytic tests do not fully probe differences in selectivity as a function of contact time. In view of this, control tests reducing the catalyst mass by a factor of 2, did not lead to any detectable change in conversion or product distribution. In contrast, increasing the flow rate by a factor of 2 decreased the relative selectivity to aromatics by about 20 %. A large increase of contact time, achieved by decreasing the flow from 88 to 8.8 mL min^{-1}, also only increased the relative aromatics selectivity by ca. 30 % when both ZSM-5 and GA/ZSM-5 were used. In all the experiments altering contact time over a wide range always produced 100 % conversion, but selectivity to aromatics only varied to a relatively low extent.

In order to study possible modifications of the zeolite structure induced by physical mixing of Ga_2O_3, XRD was used (Fig. 1). β-Ga_2O_3 was clearly detected [22], and preliminary examination of the patterns shows that the zeolite framework appears to be unaltered by Ga_2O_3 addition. In particular, the peaks at $2\theta = 45°$ and 45.6°, corresponding to the lattice planes (0 10 0) and (10 0 0) respectively, confirm that the MFI framework of the zeolite remains unmodified [23]. A more detailed examination of the XRD patterns, by determining the lattice parameters of ZSM-5 upon physically mixing with Ga_2O_3, (Table 4), revealed a contraction of the ZSM-5 unit cell volume of ca. 0.5 %, which is significant when compared to the experimental error of 0.16 %. This would suggest that even when heterogeneously mixed, crystals of β-Ga_2O_3 and ZSM-5 could interact at a more intimate level, and are not completely independent clusters. Control tests on freshly prepared physical mixtures showed a similar effect, therefore the observed phenomenon is not due to aging of the catalyst.

In contrast, the XRD pattern of the Ga/ZSM-5 catalyst prepared by WI is very similar to that of ZSM-5 (Fig. 1), and the lattice parameters are, within experimental error, identical. Finally, no reflections associated with Ga_2O_3 were detected. This is due to a Ga_2O_3 cluster size below the detection limit of the XRD method and this was confirmed by TEM (this will be discussed subsequently). It should be noted that with our preparation method for the impregnated sample, we cannot completely rule out the existence of a degree of ion exchange of Ga^{3+} with the zeolite. However, even if this should take place, it should be considered as a minor effect and the catalyst we prepared is mainly formed by Ga_2O_3 clusters supported on ZSM-5. In fact, to obtain a significant level of ion exchange saturated precursor solutions have to be used, and the ion exchange repeated under reflux several times [5, 24], which was not the case in our preparation.

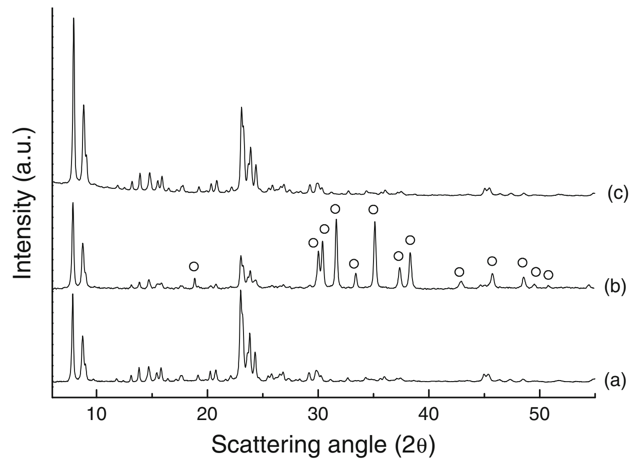

Fig. 1 XRPD patterns of: **a** ZSM-5, **b** physical mixture of Ga_2O_3 and ZSM-5 and **c** Ga/ZSM-5 obtained via wet impregnation; the *circles* identify reflections due to β-Ga_2O_3

Table 4 Lattice parameters for the zeolite ZSM-5 in ZSM-5 precursor, Ga_2O_3/ZSM-5 obtained from physical mixture and Ga/ZSM-5 obtained by wet impregnation

Sample	Structural parameters (Å)			V (Å)^3	Crystallite size (nm)
	a	b	c		
ZSM-5	20.105	19.944	13.415	5,379	61
Ga_2O_3/ZSM-5	20.090	19.898	13.385	5,351	50
Ga/ZSM-5	20.120	19.936	13.411	5,379	61

Generally, changes in selectivity due to the structure of the zeolite could also arise by a decrease in the diameter of the zeolite channel cross section by the presence of small clusters of metal oxides within the channels [25]. Clearly this cannot occur in materials prepared by physical grinding, because the crystallite size, in the range of a few µm, is several orders of magnitude larger than the channels, indicating that the interaction between Ga_2O_3 and the acid centres of the zeolite must occur on the external surface of the zeolite crystal.

This aspect was investigated further by preparing physical mixtures comprising Ga_2O_3 and zeolite H-β. Control tests using Ga_2O_3/H-β showed that the presence of Ga_2O_3 still enhances the selectivity to aromatics from ca. 18 to 30 % (Tables 5, 6), although a higher amount of dimethylether (DME) was also detected. This enables the effect of the zeolite structure to be investigated, because zeolite ZSM-5 is a pentasil phase consisting of two

Table 5 Methanol conversion over H-β (SiO_2:Al_2O_3 = 38:1)

Time (min)	Selectivity (wt%)											Total aromatics
	C_2	C_3	C_4	C_5	C_6+	C_6H_6	C_7H_8	C_8H_{10}	C_9H_{12}	$C_{10}H_{14}$	$C_{11}H_{16}$	
34	10.0	18.1	38.1	10.9	4.5	0.0	0.6	0.9	2.3	9.6	5.0	18.4
120	10.0	20.7	37.7	11.7	6.2	0.1	0.8	0.9	1.0	5.0	6.0	13.7
151	9.5	20.3	37.0	11.8	6.5	0.1	0.8	0.8	0.8	3.7	8.8	15.0
188	9.8	21.2	37.5	12.0	7.0	0.1	1.0	0.8	0.7	2.3	7.7	12.5
232	9.9	21.7	38.0	12.4	7.5	0.1	0.7	0.8	0.6	1.6	6.8	10.5
266	9.8	21.4	37.3	12.2	7.6	0.1	0.8	0.8	0.6	1.3	8.0	11.6
323	10.3	21.6	38.1	12.7	8.0	0.1	0.8	0.8	0.6	1.1	6.1	9.4

Table 6 Methanol conversion over β-Ga_2O_3/H-β (SiO_2:Al_2O_3 = 38:1) physical mixture

Time (min)	Selectivity (wt%)												Total aromatics
	C_2	C_3	C_4	C_5	C_6+	C_6H_6	C_7H_8	C_8H_{10}	C_9H_{12}	$C_{10}H_{14}$	$C_{11}H_{16}$	DME	
32	24.5	18.7	21.0	4.4	0.8	0.0	0.7	0.9	1.3	5.2	22.3	0.0	30.4
68	19.8	18.9	24.8	6.4	2.3	0.0	1.4	1.4	2.2	12.0	9.8	1.0	26.8
101	20.5	21.2	22.7	6.7	3.4	0.1	1.5	1.4	0.9	3.2	12.9	5.5	20.0
159	18.3	18.2	21.2	7.2	3.4	0.1	1.4	1.2	0.8	3.8	10.1	14.3	17.4
190	12.8	13.6	12.2	5.6	2.7	0.1	0.8	1.0	0.6	1.4	12.2	36.9	16.1
235	9.7	10.2	11.3	4.6	2.1	0.1	0.4	0.7	0.4	0.9	12.7	46.7	15.4
301	7.6	7.5	4.3	3.8	1.2	0.1	0.3	0.6	0.3	0.6	9.2	64.5	11.0

perpendicular intersecting channel systems having cross sections of 5.4 × 5.6 and 5.1 × 5.4 Å [26], and rings made of 10 T-atoms units, while zeolite-β has rings of 12 T-atoms with a size of 6.8 Å. This affects the selectivity to aromatics, regardless of the different acidic nature of the zeolite used, as zeolite-β is capable of promoting the formation of alkenes, such as isobutene [27], which could be involved in the dehydrogenation process leading to aromatics [18]. This suggests that in this case formation of aromatics was the result of a dehydrogenation reaction of the alkenes, induced by Ga_2O_3 clusters.

The reducing effect of Ga_2O_3 is certainly not unprecedented, and at present, the preparation and use of physical mixtures of Ga_2O_3 and ZSM-5 has found application for other reactions, such as the conversion of NO_2 to N_2 [28]. For this reaction, the physical mixture was also more active than the additional effect of the two individual components, Ga_2O_3 and ZSM-5, and using a mixture with Na-ZSM-5 suppressed activity, suggesting a cooperative effect involving the zeolite acid sites.

This same type of effect could help to explain the reactivity we observe in the present study. In the case of methanol to hydrocarbon conversion the acid sites of the zeolite are known to be responsible for the initial dehydration of methanol to DME and then to aromatics [1]. Hence, the activity of the Ga/ZSM-5 catalysts, either a physical mixture of Ga_2O_3 and ZSM-5 or an impregnated catalyst comprising Ga_2O_3 crystals at the edge of ZSM-5, would be the result of a contact synergy [11, 29] between the basic Lewis centres of Ga_2O_3 and the Brønsted acid sites of the zeolite, an effect previously reported for mixtures of $MnMoO_4$ and MoO_3 for the oxidation of C_4 hydrocarbons [30]. Conversely, conventional impregnation and calcination processes would lead to the formation of segregated β-Ga_2O_3 particles on the external surface of the zeolite crystals, and no direct shape selectivity control over the final product distribution should be possible [31] Therefore, in order to explain the enhanced formation of aromatics, we should consider the importance of removal of hydrogen from the reaction sites by Ga_2O_3 [13, 32]. In fact, independently from the overall reaction mechanism considered for the aromatization process, aromatics are mainly formed by dehydrocyclization reactions of alkenes [33], and the metal oxide would assist this process by promoting the removal of hydrogen as H_2 [34] enhancing selectivity. A similar effect has been observed in the dehydro-oligomerization of methane to aromatics over Mo/ZSM-5 catalyst [35]. Our data support this process for all the physical mixtures tested, since there is very little CH_4 (<1 %) and the C_2–C_5 hydrocarbons identified are all essentially alkenes. Therefore, in order to obtain aromatic products, H_2 must be formed [34]. This was confirmed by

Table 7 Concentration of H_2 in the exit stream for physical mixtures of (a) β-Ga_2O_3/H-ZSM-5 and (b) β-Ga_2O_3/H-β

Time (min)	32	60	91	127	158	193	223	253	294
H_2 conc/vol.%^{a}	1.9	1.9	1.9	1.9	1.9	1.9	1.9	1.8	1.9
H_2 conc/vol.%^{b}	0.9	2.0	2.8	3.6	3.7	4.1	4.2	4.1	4.2

analyzing the reactor effluents and an accurate quantification of the H_2 content for physically mixed Ga_2O_3/ZSM-5 was carried out for the first time (Table 7). H_2 was in the range 1.5–1.9 %, whilst for gallium H-β zeolite, H_2 formation was up to 4 %. It should also be noted that no CO or CO_2 were detected at any stage of the reaction, and a carbon mass balance >90 % was measured. This is also similar to the aromatization of propene in the Cyclar process [36], which is also catalyzed by Ga/ZSM-5 above 600 °C.

Transmission electron microscopy was carried out for the samples prepared by WI before and after reaction, with the aim of obtaining information on morphology and coke deposition. In BF TEM images (Fig. 2), the Ga_2O_3 clusters display darker contrast against the lighter ZSM-5 support due to their higher average atomic number. Electron microscopy analysis of the fresh Ga/ZSM-5 catalyst prepared by wet impregnation shows that the Ga_2O_3 particles are not very well dispersed (highlighted with cyan in Fig. 2a) and the majority of the sample has Ga_2O_3 agglomerates with relatively uncovered ZSM-5 support. Only a small fraction of the ZSM-5 support could be found in this sample that had highly dispersed Ga_2O_3 clusters over the surface (Fig. 2b, highlighted in red). However, we consider the real breakthrough in understanding the catalyst behaviour was obtained by analyzing the samples by TEM after reaction (Fig. 2c, d). After reaction the Ga/ZSM-5 sample prepared by WI displays a much improved

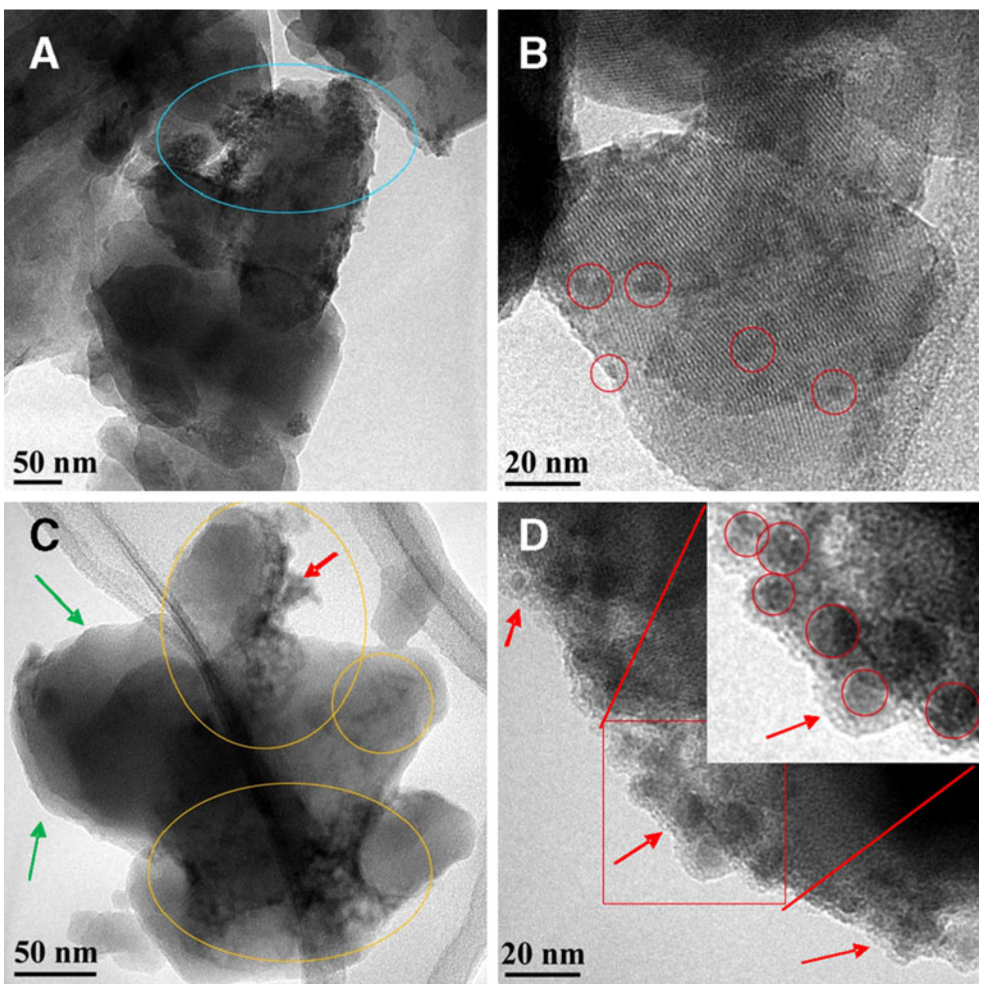

Fig. 2 Representative BF-TEM micrographs of Ga/ZSM-5 prepared via wet impregnation (WI-01); **a**, **b** micrographs of the sample before reaction and **b**, **d** after reaction. The *red circles* highlight some of dispersed Ga_2O_3 clusters on ZSM-5 surface. The *red arrows* point to the coke layers on the Ga_2O_3/ZSM-5 interface; the *green arrows* point to coke-free ZSM-5 surface that is remote from Ga_2O_3 particles

Ga_2O_3 dispersion on the ZSM-5 surface compared with the fresh catalyst, which indicates an increase in the contact surface area between the Ga_2O_3 clusters and ZSM-5. The Ga_2O_3 clusters are not homogenously distributed on the ZSM-5 surface, but often form network structures that are embedded in deposits of coke (Fig. 2c, d). Coke is preferentially deposited on the dispersed Ga_2O_3 particles to a thickness of 1–5 nm (highlighted by red arrows), whilst the ZSM-5 surface remote from the Ga_2O_3 is again relatively carbon free (indicated by green arrows in Fig. 2c). Coke deposition most likely inhibits large molecules from reaching/leaving the Ga_2O_3/ZSM-5 interface region, thereby leading to the changes in the selectivity and activity of the catalyst we observe.

The Ga_2O_3/zeolite interface region is the probable location of the catalyst active sites for the methanol to aromatics reaction. When this interface is covered by coke (ca. 5 % wt.) the catalyst show a decrease of aromatic selectivity from 50 to 40 % and increased methane formation, up to 5 %, suggesting cracking of coke products [37] or methylation reactions [3].

It should be stressed that also coke is a consequence of dehydrogenation reactions [38], and in our case this is predominantly found at the edge of Ga_2O_3 crystals rather than the zeolite function. This experimental evidence can be considered a further proof of the mechanism of action of Ga_2O_3 clusters we proposed. As Ga_2O_3 displays enhanced dehydrogenation properties, therefore leading to aromatics via reaction outside the pore channels, this in turn can also enhance the presence of coke outside the zeolite function.

There is in fact, a correlation between loss of selectivity to aromatics and coke formation on the catalyst and this is also accompanied by a corresponding increase of light hydrocarbons, such as propene, which are known to be precursors for forming aromatics [6, 39]. Therefore it follows that the greater the extent that the gallium oxide zeolite interfacial active sites are blocked, aromatic formation is inhibited, and the products shift towards light hydrocarbons. For example, in the case of propene there was an increase from 8 to 12 %. In view of these effects, it is likely that the enhanced aromatization obtained by non framework species, like the catalysts used in this study, is due to enhanced removal of hydrogen from the reaction site thus promoting the formation of aromatic products.

Finally the deposition of coke on the catalyst during reaction is not ideal, but inevitable during the methanol to aromatics reaction. Hence it is important to probe catalyst regeneration. Studies carried out in flowing air showed that he WI catalyst could be treated at 550 °C (12 h, air flow 60 mL min^{-1}) to oxidise carbonaceous deposits. After the thermal treatment it was possible to recover fully the initial activity and product selectivity observed for the fresh catalyst. Furthermore, it was possible to repeat the regeneration process for a number of cycles without observing any loss of catalyst performance.

4 Conclusions

It has been observed that Ga_2O_3 crystallites were able to enhance the selectivity to aromatics from methanol, particularly for the C_6–C_8 products. In particular, physical mixtures of Ga_2O_3 and ZSM-5 indicate that it is the interface on the external surface of the zeolite crystal which controls selectivity. Despite the existence of efficient gallium based catalysts for the methanol to aromatics reaction [40, 41], we consider these results to be important for catalyst design. In fact, they show that as well as the major role associated with shape selective catalysis typical of zeolitic materials, it is possible to drive enhanced selectivity to aromatics by introducing chemical species, like Ga_2O_3 nanoparticles, outside of the zeolite channels, thus providing an additional tunable parameter for the design of zeolite-based catalysts with the desired characteristics.

Acknowledgments The authors thank SABIC for financial support.

References

1. Corma A (1997) Chem Rev 97:2373
2. Klyueva NV, Tien ND, Ione KG (1985) React Kinet Catal Lett 29:427
3. Hutchings GJ, Gottschalk F, Hall MVM, Hunter R (1987) J Chem Soc, Faraday Trans 1(83):571
4. Kumar N, Lindfors LE (1996) Catal Lett 38:239
5. Fricke R, Kosslick H, Lischke G, Richter M (2000) Chem Rev 100:2303
6. Conte M, Lopez-Sanchez JA, He Q, Morgan DJ, Ryabenkova Y, Bartley JK, Carley AF, Taylor SH, Kiely CJ, Khalid K, Hutchings GJ (2012) Catal Sci Technol 2:105
7. Hashimoto S, Uwada T, Masuhara H, Asahi T (2008) J Phys Chem C 112:15089
8. Serykh AI, Amiridis MD (2009) Surf Sci 603:2037
9. Price GL, Kanazirev V (1990) J Catal 126:267
10. Frash MV, van Santen RA (2000) J Phys Chem A 104:2468
11. Hagen A, Roessner F (2000) Catal Rev 42:403
12. Yoshio O, Hiroshi A, Yoko S (1988) J Chem Soc Faraday Trans 1(84):1091
13. Csicsery SM (1986) Pure Appl Chem 58:841
14. Freeman D, Wells RPK, Hutchings GJ (2001) Chem Commun 1754
15. Mao R, Yao J, Sjiariel B (1990) Catal Lett 6:23
16. Badran AH, Dwyer J, Evmerides NP (1997) Inorg Chim Acta 21:233
17. Cullity BD, Stock SR (2001) Elements of X-ray diffraction, 3rd edn. Prentice-Hall Inc, Upper Saddle River
18. Kanai J, Kawata N (1990) Appl Catal 62:141
19. Dwyer FG, Hanson FV, Schwartz AB (1977) US Patent 4,035,430
20. Chang CD, Lang WH (1977) US Patent 4,013,732
21. Olah GA, Molnár Á (2003) Hydrocarbon chemistry, 2nd edn. Wiley, Hoboken

22. International Centre for Diffraction Data, Powder Diffraction File, Entry 41-1103 (1996)
23. Mansour R, Lafjah M, Djafri F, Bengueddach A (2007) J Kor Chem Soc 51:178
24. Choudhary VR, Kinage AK (1995) Zeolites 15:732
25. Quian L, Yan ZF (2001) Colloids Surf A 180:311
26. Bleken F, Skistad W, Barbera K, Kustova M, Bordiga S, Beato P, Lillerud KP, Svelle S, Olsbye U (2001) Phys Chem Chem Phys 13:2539
27. Hutchings GJ, Johnston P, Lee DF, Warwick A, Williams CD, Wilkinson M (1994) J Catal 47:177
28. Kikuchi E, Ogura M, Terasaki I, Goto Y (1996) J Catal 161:465
29. Freeman D, Wells RPK, Hutchings GJ (2002) J Catal 205:358
30. Ozkan S, Smith MR, Driscoll SA (1992) Stud Surf Sci Catal 72:363
31. Lalik E, Liu X, Klinowski J (1992) J Phys Chem 96:805
32. Bayense CR, van Hoff JHC, Kentgens APM, de Haan JW (1989) J Chem Soc Chem Commun 1292
33. Weckhuysen BM, Wang D, Rosynek MP, Lunsford JH (1998) J Catal 175:338
34. Iglesia E, Baumgartner JE, Price GL (1992) J Catal 134:549
35. Chen LY, Lin LW, Xu ZS, Li XS, Zhang T (1995) J Catal 157:190
36. Buckles G, Hutchings GJ, Williams CD (1991) Catal Lett 11:89
37. Haag WO, Lago RM, Rodewald PG (1982) J Mol Catal 17:161
38. Nedomová K, Wichterlová B, Beran S, Bednárová S (1988) Catal Today 3:373
39. Popova Z, Aristirova K, Dimitrov C (1990) React Kinet Catal Lett 41:369
40. Mowry JR, Anderson RF, Johnson JA (1985) Oil Gas J 83:1288
41. Doolan C, Pujado PR (1989) Hydrocarbon Proc 68:72